

# Evaluation of Electromagnetic Field Distributions under 1.5 T MRI Scanning Within Human Models of a Virtual Family

Yan Liu<sup>1</sup>, Dawei Li<sup>1</sup>, Xiaoyi Min<sup>2</sup>, Shiloh, Sison<sup>2</sup>, Gabriel Mouchawar<sup>2</sup>, Ji Chen<sup>1</sup>

<sup>1</sup>University of Houston, Houston, USA

<sup>2</sup>St. Jude Medical, Sylmar, USA

## Abstract

*Magnetic Resonance Imaging (MRI) has been contraindicated in patients with pacemakers or implantable cardioverter-defibrillators (ICDs) due to safety concerns, such as the heating of adjacent bodily tissue due to radio frequency (RF) induced current. The ISO/IEC 10974 Joint Working Group (JWG) has developed a tiered approach in establishing the worst case RF heating conditions that active implantable devices may experience during MRI utilizing computer simulations. According to the ISO/IEC JWG tier 2 approach, we evaluated the electric fields induced in the implant regions of pacemakers and ICDs in five human body models during 1.5 T MRI scans. The maximum electrical field (Emax) can be used as a conservative estimation to test MRI induced heating.*

*The SEMCAD software package was used to calculate the electric field distribution due to RF fields from high pass and low pass MRI birdcage coils. The variables studied in the simulations also included circularly polarized field rotations, body positions inside RF coils (landmark positions), tissue properties, and RF coil size. The Emax and 95<sup>th</sup> percentile electric field values were computed from the simulations at each of multiple implant regions.*

## 1. Introduction

With the increased use of implantable medical devices, there have been concerns related to the interaction between magnetic resonance imaging (MRI) systems with these devices. These interactions include magnetic field interactions, heating, and image artifacts [1]. Notably, MRI-related heating may lead to tissue damage near implants that have elongated metallic components. Accordingly, MRI safety issues are generally characterized by following standards. Such standards are based on those appropriate test procedures presented by the International Organization for Standardization and the International Electrotechnical Commission (ISO/IEC) and

American Society for Testing and Materials (ASTM) International [2].

The ISO/IEC Joint Working Group (JWG) has developed a four-tiered approach utilizing computer simulations to estimate the electric fields to predict the RF heating caused by active implantable devices during MRI scans. The lower the tier, the more conservative the estimate is. Tier 2 utilizes either Emax or the 95th percentile electric field in the region of the implanted system in human body models for estimating RF heating. The simulated Emax (or the 95th percentile value) may then be used to set an incident electrical field on a device under testing in an in vitro test set up for estimating the worst case RF heating.

We carried out the tier 2 approach by identifying the Emax in the pacemaker/ICD region through simulations in five different-sized human body models, each tested with various material parameters. Additional simulated variable conditions included the human body types inside high pass and low pass RF coils, circularly polarized field rotations, human body tissue properties, body positions inside RF coils, and different RF coil sizes.

## 2. Material and method

Five body models were used from the Virtual Population Project: obese male (Fats), adult male (Duke), adult female (Ella), girl (Billie), and boy (Thelonius) as shown in Fig. 1[3][4]. The SEMCAD X software package [5] was used to simulate the electric fields generated throughout the human body when exposed to electromagnetic energy generated by an MRI RF body coil. SEMCAD X uses Finite-Difference Time-Domain (FDTD) methods to iteratively compute the electric and magnetic fields. The models have a meshed spatial resolution of 2 mm X 2 mm X 2 mm.

For the model of the RF body coil in 1.5 T MRI systems, the simulation frequency was set to 64 MHz and the coil with its shield was included in the model. After solutions were obtained, these electric fields were then processed inside the implant regions with 10 gram average in order to eliminate computation artifacts [6]. All the

reported electric fields in root-mean-square values were scaled to 4 W/kg or 2 W/kg for whole-body averaged SAR, or 3.2 W/kg for head SAR limit.

SEMCAD X models of 16 rung copper circularly polarized high-pass and low-pass RF body coils [7] were created. For the high-pass RF body coil an ideal source (red cones in Fig. 2) was inserted in the end rings between each rung. The amplitude of each source was set to 1 V for the  $n$ th sources and -1 V for the  $n$ 'th sources. The phase delay of both the  $n$ th and  $n$ 'th sources was set to  $n/16$ . For the low-pass RF body coils, an ideal source was inserted in the rung half way along its length. The amplitude of each source was set to 1 V and the phase delay of the  $n$ th source was set to  $n/16$ . Modeling the sources this way forces the current to that of an ideal circularly polarized RF body coil [8]. The ideal or 'accelerated' RF body coil model reduces the simulation time and eliminates the need for tuning, as necessary with non-ideal models containing capacitors.

Each simulation was completed once the electric field distribution in the simulation domain converged (this typically requires a simulation time of 20-30 periods of the RF signals). The simulation boundaries were enclosed by the Uniaxial Perfectly Matched Layer Absorbing Boundary Condition (UPML ABC) so that impinging waves would not reflect back into the computational domain.

Once the simulation was finished the whole body SAR and the head SAR were calculated with input power of 1 W. In this process all but the RF body coil and shield were included in the SAR calculation.

Based on the whole body SAR and the head SAR obtained at an input of 1 W, normalization factors were determined to achieve a whole body SAR of 4 W/kg or 2 W/kg as well as the head SAR of 3.2 W/kg. The normalization factors were used to scale  $E_{max}$  with the conditions of the whole body SAR of 4 W/kg or 2 W/kg and the head SAR of 3.2 W/kg. In applying a head SAR limit of 3.2 W/kg, we selected the smaller  $E_{max}$  value of those between the whole body SAR and the head SAR.

The variable conditions simulated included five human body types, high pass and low pass RF coils, circularly polarized field rotations (counter clockwise and clockwise), body positions inside the RF coils (landmark positions), bodily tissue properties, and RF coil size. The simulations began with an investigation into the largest  $E_{max}$  values generated in the pacemaker/ICD region within all five body models with all other "nominal" conditions. In order to determine the effect of body position along the Z-axis (shifting the body in the supine position within the coil along the head-foot dimension), the five body models were simulated at multiple positions at 10 cm steps. Next, we determined the effect of shifting the body to various X (shifting the body along the left-right dimension) and Y (shifting the body along the front-back dimension) positions.

The effect of tissue conductivity was studied by varying the conductivities of 46 bodily tissues within the model by  $\pm 20\%$  relative to their nominal conductivities, maintaining other conditions nominally. Due to space limitations, these data are not reported here. Lastly, the effect of coil type and size was studied, maintaining the other conditions nominally.

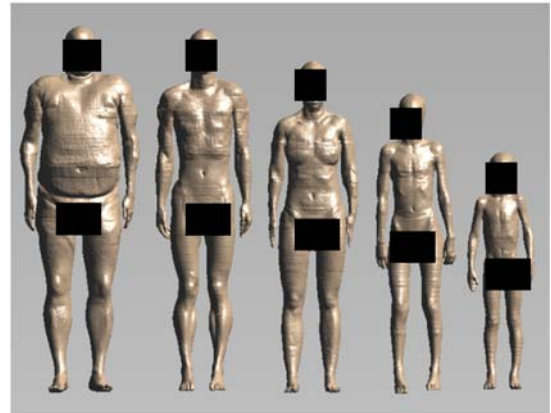


Fig. 1. Illustration of the five body models used in this study.

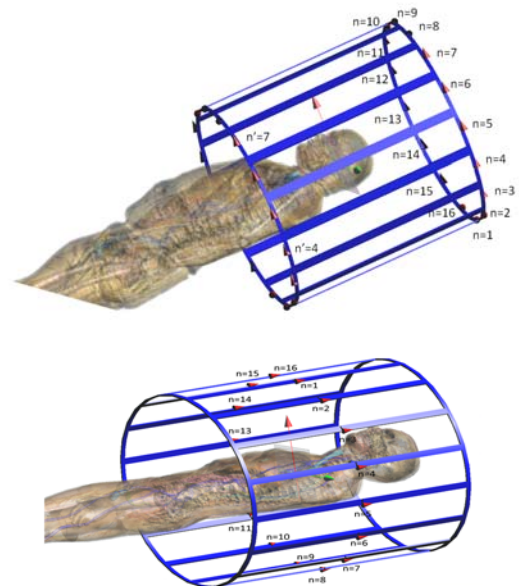


Fig. 2. Illustration of RF coils and loading in simulations.

In each of the five body models, six sub-regions along the hypothetical pathway of a lead attached to a pacemaker/ICD were constructed as shown in Fig. 3. These sub-regions are named: heart, superior vena cava (SVC), left jugular vein, right jugular vein, left pectoral region, and right pectoral region. The maximum electric fields in each region were identified from each simulation.

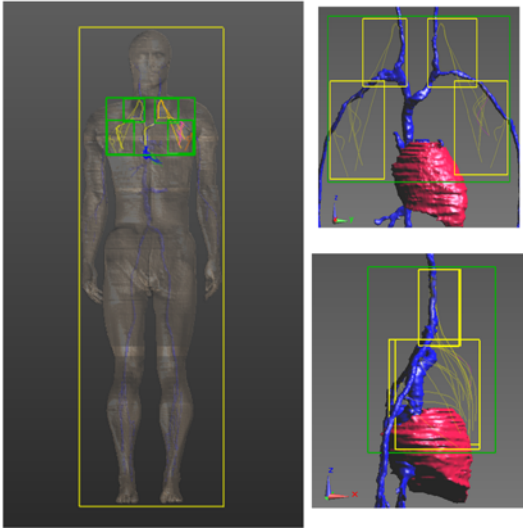


Fig. 3. Illustration of the pacemaker/ICD sub-regions defined in the adult male body model.

### 3. Results and discussion

#### 3.1. Effect of body model and Z-axis landmark position

Fig. 4 shows the maximum electric fields induced over all of the implant sub-regions in the five human body models as the models are situated at various Z-axis body positions. The largest values are seen in the obese male model, with a Z-axis position between 0 cm and 20 cm. This agrees with expectations, as the obese model is nearest to the RF coil, and is therefore expected to have the highest  $E_{max}$ . This also agrees with recent literature indicating that the peak spatial SAR [9] and electric field [10] are highest with the obese model.

Fig. 5 shows the maximum electric fields in different sub-regions of the obese model at various model landmark positions. In most loading positions, the left jugular vein region experienced the highest electric field. As the obese model is positioned farther away from the coil, the maximum electric field location shifts to the left pectoral region. However, the overall maximum electric field over the entire implant region is at the left jugular vein when the human body is loaded at the 10 cm landmark position.

#### 3.2. X- and Y-axis loading position

The maximum  $E_{max}$  within the implant regions for each simulation with the obese model at various X, Y, and Z positions is shown in Fig. 6.

Analysis of the Z-axis simulations which generated the largest  $E_{max}$  (at  $Z = 10$  cm) shows that the absolute maximum occurs when the obese model was raised by 5 cm in the Y direction (0 cm, 5 cm, 10 cm). The variation

in  $E_{max}$  between these tested loading positions' maximum to minimum was about 25%.

The effects of RF coil type, coil length and diameter, and the electromagnetic parameters such as conductivity, relative permeability and permittivity of the human tissue are also investigated. With the consideration of all those factors mentioned above, 218 simulations in total are simulated and analyzed. Due to the context limitation, the details of their effects are not included here.

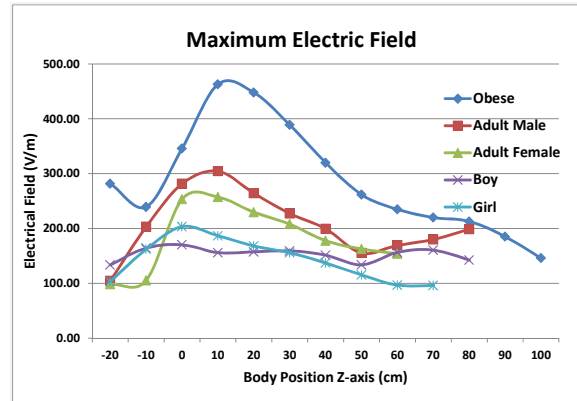


Fig. 4. Computed maximal electric field values within the pacemaker ICD implant regions with different body models at different landmark positions. (Whole body SAR Limit (2 W/kg) and Head SAR Limit (3.2 W/kg)).

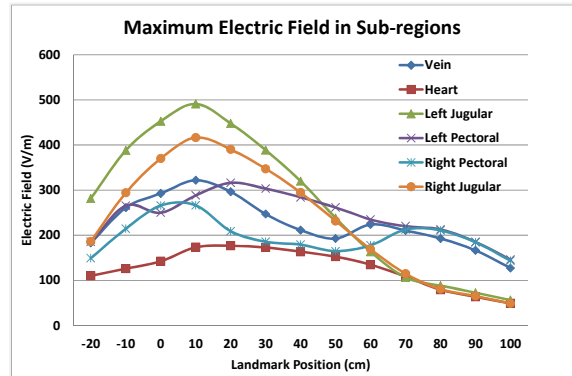


Fig. 5. Extracted electric field values of the obese model at different landmark positions. (Whole body SAR Limit (2 W/kg) and Head SAR Limit (3.2 W/kg)).

Through these extensive electromagnetic simulations, the histogram of maximum electric fields for all the human body types tested is shown in Fig. 7. The maximum electric field value is 639 V/m, while the 95<sup>th</sup> percentile is 568 V/m. For each sub-region, the maximum and 95<sup>th</sup> percentile electric field scaled to different SAR limits is shown in Table 1.

### 4. Summary and conclusion

We simulated 5 different human body models undergoing 1.5 T MRI scanning under various conditions

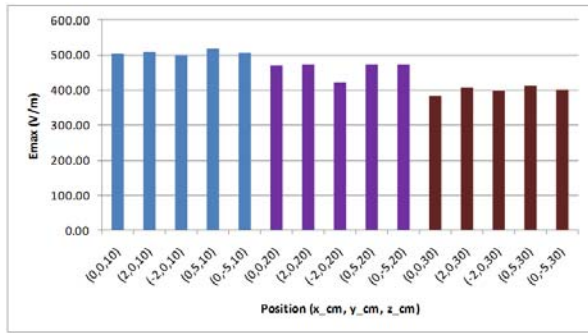


Fig. 6. Computed electric field values at different X, Y, and Z landmark positions for the obesity model.

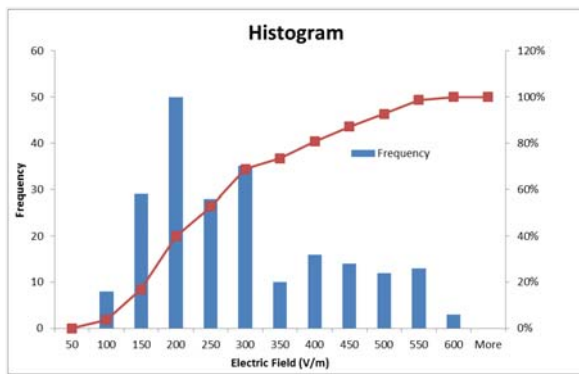


Fig. 7. Histogram of Emax distribution.

Table 1 Maximum Electric Field in Each Sub-region (V/m)

Implant Region	Whole body SAR Limit (4 W/kg) and Head SAR Limit (3.2 W/kg)		Whole body SAR Limit (2 W/kg) and Head SAR Limit (3.2 W/kg)	
	Maximum	95 <sup>th</sup> percentile	Maximum	95 <sup>th</sup> percentile
SVC	522.7	447.4	474.7	359.2
Heart	267.9	248.6	219.2	192.7
Left Jugular	639.4	563.5	582.2	508.0
Right Jugular	630.4	522.1	511.1	459.7
Left Pectoral	554.9	455.9	491.7	358.8
Right Pectoral	592.0	483.0	436.4	380.4
Maximum	639.4	568.4	582.2	511.1

in order to identify the maximum electric field in the region of an implanted pacemaker or ICD. In general, the electric fields induced were greater the larger the body model. The greatest induced electric fields scaled to different SAR limits are shown in Table 1. With the whole body SAR of 2 W/kg and a head SAR limit of 3.2 W/kg, the overall highest Emax was 582 V/m, and it was

found at a body position within the coil at X = 0 cm, Y = 5 cm, and Z = 10 cm. The 95<sup>th</sup> percentile of electric field was 508 V/m. With the whole body SAR of 4 W/kg and the head SAR limit of 3.2 W/kg, the overall highest Emax was 639 V/m, found in the jugular region with the body position within the coil at X = 2 cm, Y = 0 cm, and Z = 10 cm. In this case, the 95<sup>th</sup> percentile of electric field is 563 V/m. The lowest electrical fields we observed were generally within the heart.

The overall Emax or the 95<sup>th</sup> percentile of electrical field values may be used as overly conservative criteria in assessing the RF heating that a pacemaker or an ICD may experience under MRI scanning. The Emax values identified in this analysis in certain sub regions may also be used to estimate the worst case RF heating during MRI scanning that small leadless devices might bear.

## References

- [1] Wood TO. Standards for medical devices in MRI: present and future. | Journal of Magn Reson Imaging 2007; 26: 1186-1189.
- [2] ASTM International. Standard test method for measurement of radio frequency induced heating near passive implants during magnetic resonance imaging. ASTM standard F2182-11 West Conshohocken, PA: ASTM International: 2011.
- [3] Christ A, Kainz W, Hahn EG, Honegger K, Zefferer M, Neufeld E, Rascher W, Janka R, Bautz W, Chen J, Kiefer B, Schmitt P, Hollenbach HP, Shen J, Oberle M, Szczerba D, Kam A, Guag JW, Kuster N. The virtual family – development of surface-based anatomical models of two adults and two children for dosimetric simulations. Physics in Medicine and Biology 2009;55:N23-N28.
- [4] IT'IS 2010 Virtual Population Project <http://www.itis.ethz.ch/research/virtual-population/virtual-population-project/>
- [5] SEMCAD X Reference Manual, SEMCAD Simulation Platform for Electromagnetic Compatibility.
- [6] IEC 60601-2-33:2002(E) Particular requirements for the safety of magnetic resonance equipment for medical diagnosis.
- [7] Jin J. Electromagnetic Analysis and Design in Magnetic Resonance Imaging. Boca Raton, FL: CRC Press, 1998.
- [8] Hayes C. Radio frequency field coil for NMR. U.S. Patent #4,694,255, Sept. 15, 1987.
- [9] Neufeld E, Gosselin M-C, Murbach M, Christ A, Cabot E, Kuster N. Analysis of the local worst-case SAR exposure caused by an MRI multi-transmit body coil in anatomical models of the human body. Physics in Medicine and Biology 2011;56: 4649-4659.
- [10] ISO/TS 10974:2012(E) Assessment of the safety of magnetic resonance imaging for patients with an active implantable medical device.

Address for correspondence.

Ji Chen, [jchen23@Central.UH.EDU](mailto:jchen23@Central.UH.EDU)  
 Dept. of Electrical & Computer Engineering  
 N308 Engineering Building 1, Houston, Texas 77004-4005